VARIABILITY OF THE SOLAR NEUTRINO FLUX

David Caldwell - *UC Santa Barbara*

Jeff Scargle - *NASA Ames Research Center*

Peter Sturrock, Guenther Walther - *Stanford University*

Mike Wheatland - *Sydney University*

S0306A06

SOLAR NEUTRINO PROBLEM
STANDARD INTERPRETATION

Standard Solar Model

Neutrinos of Majorana type

Effectively zero magnetic moment

Flux Reduction due to Flavor Oscillation [MSW Effect]

Depends upon density

Independent of magnetic field

Since the solar density is spherically symmetric, the detected neutrino fluxes should be constant

Time Variation is Incompatible with this Theory

VARIABILITY TESTS

1. Look for correlation between measured flux and some solar index such as sunspot number

2. Examine variance of measurements, in comparison with simulations

3. Examine histograms of measurements, in comparison with simulations

4. Look for oscillations that can be identified with known solar oscillations

Only #4 makes full use of the timing data

SOLAR PERIODICITIES

Hale cycle	22 years	0.046 cpy
Sunspot cycle	11 years	0.09 cpy
Howe oscillation	1.3 years	0.77 cpy
Rieger oscillation	156 days	2.34 cpy
Rieger-type oscillations	78 days	4.68 cpy
	52 days	7.02 cpy

Internal rotation - equatorial (sidereal)

Radiative zone	13.9 +/-0.5 cpy
Tachocline	13.7 to 14.6 cpy
Convection zone	14.2 to 14.9 cpy

Internal rotation - equatorial (synodic)

Radiative zone	12.9 +/-0.5 cpy
Tachocline	12.7 to 13.6 cpy
Convection zone	13.2 to 13.9 cpy

Plus harmonics of rotation rate

SOLAR NEUTRINO FLUX VARIABILITY

AVAILABLE DATA SETS

• Homestake	[Radiochemical - Chlorine]
• GALLEX-GNO	[Radiochemical - Gallium]
• SAGE	[Radiochemical - Gallium]
• Super-Kamiokande	[Cerenkov]

SOLAR NEUTRINO FLUX VARIABILITY

NOT YET AVAILABLE DATA SETS

- Kamiokande, Kamiokande II [Cerenkov]
- Sudbury Neutrino Observatory [SNO, Cerenkov]

S0205B13

GALLEX AND GNO DATA ANALYSIS

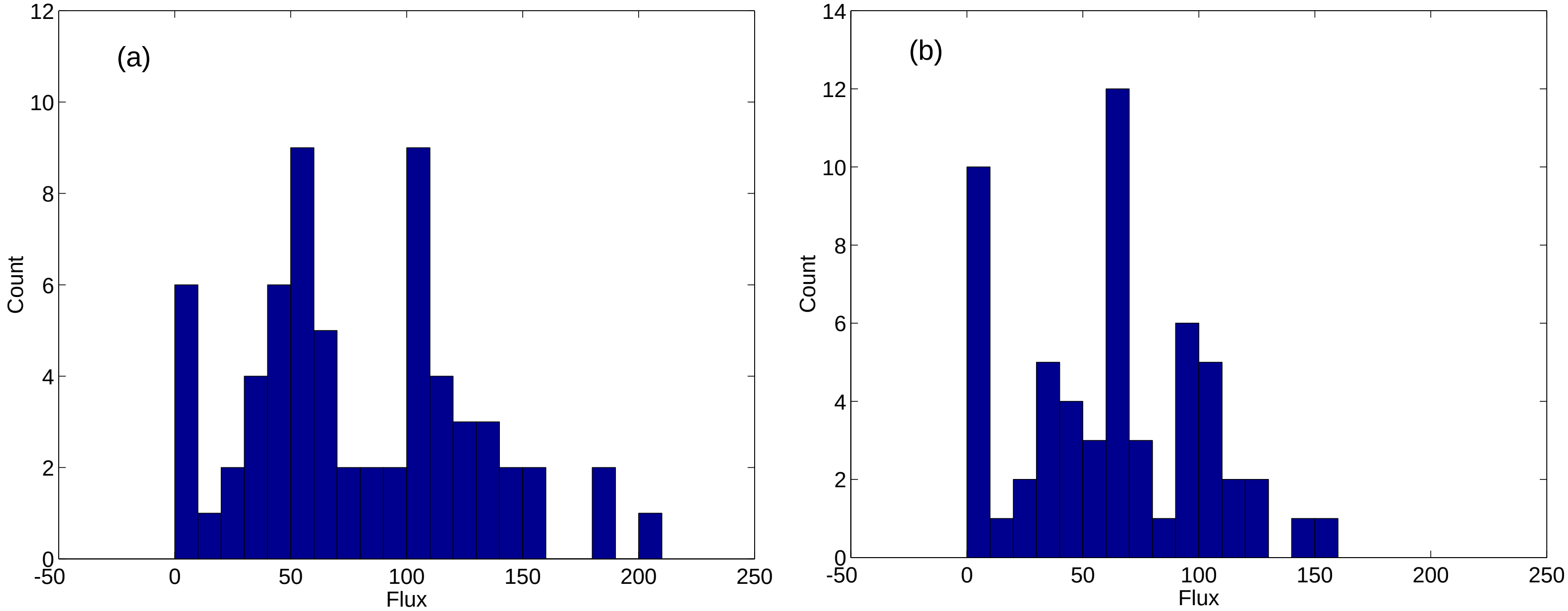

Histograms of flux values for (a) Gallex, and (b) GNO.

GALLEX AND GNO DATA ANALYSIS

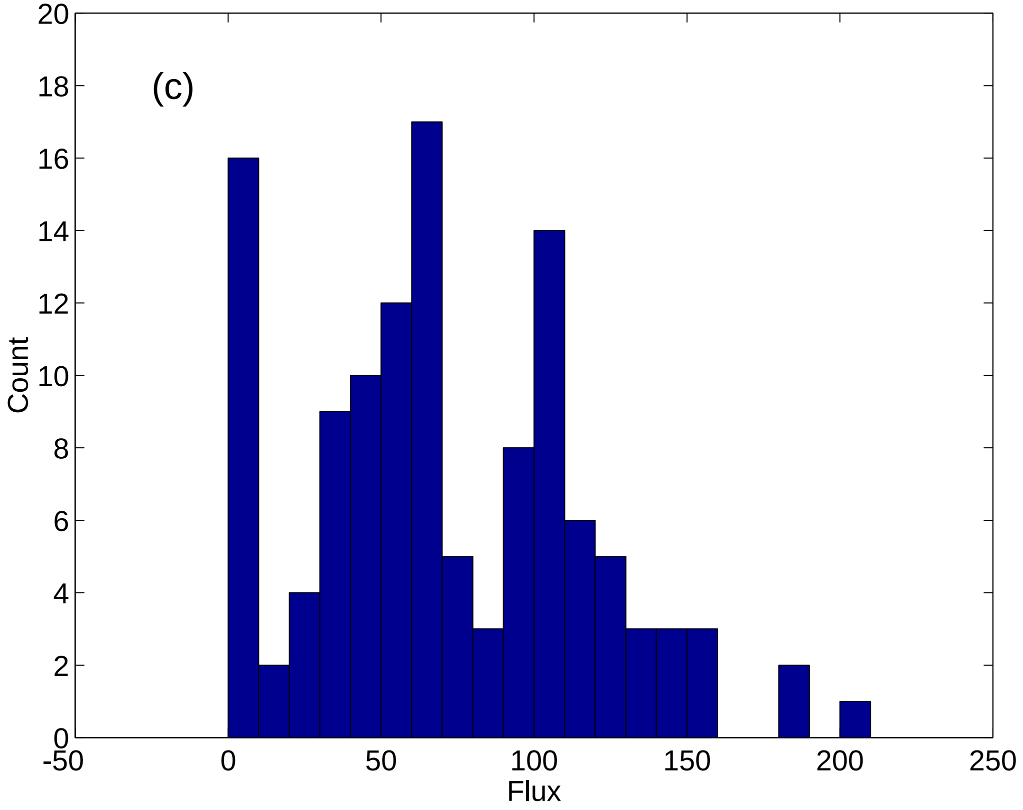

Histogram of flux values for Gallex and GNO combined

GALLEX AND GNO DATA ANALYSIS

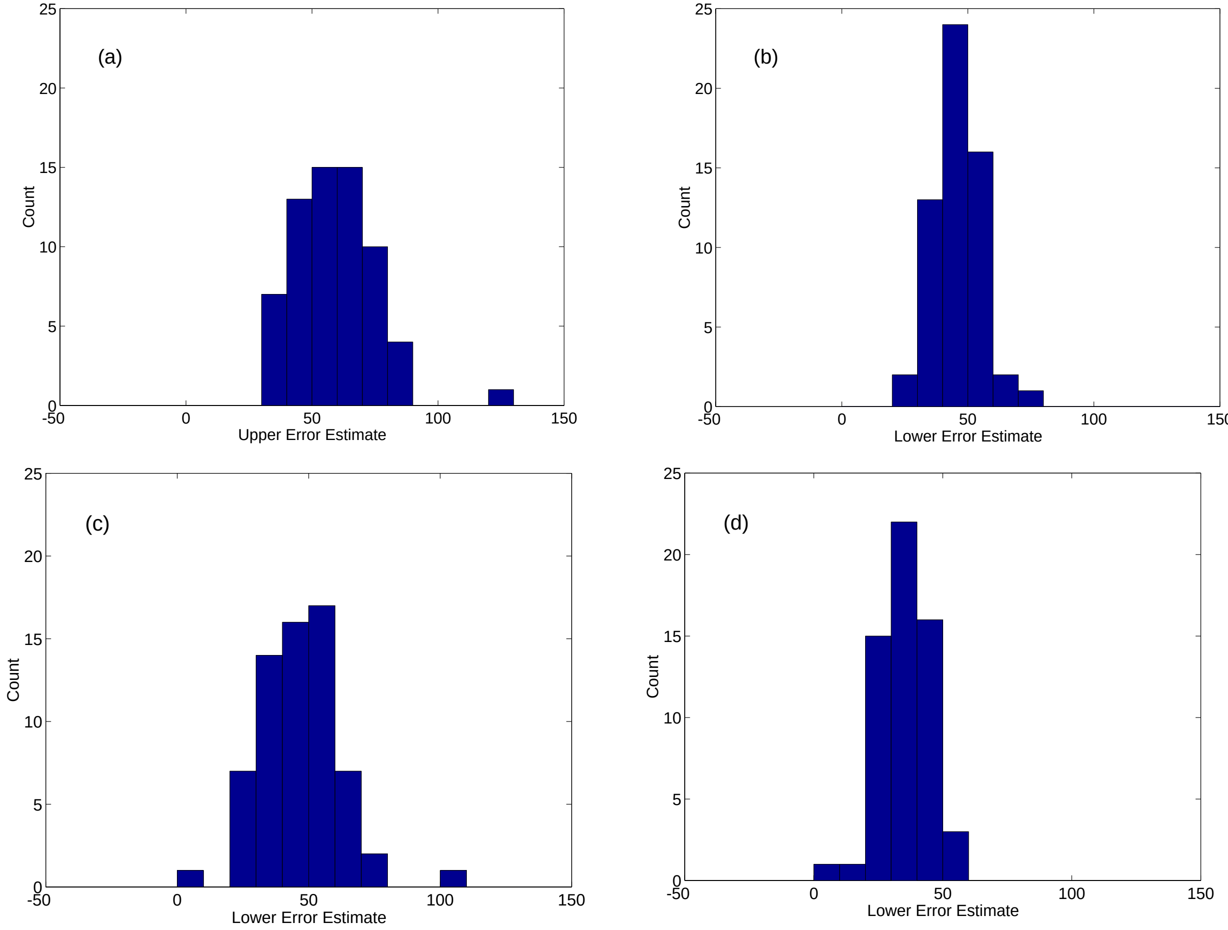

Histograms of (a) su for Gallex, (b) su for GNO,
(c) sl for Gallex, (d) sl for GNO.

GALLEX AND GNO DATA ANALYSIS

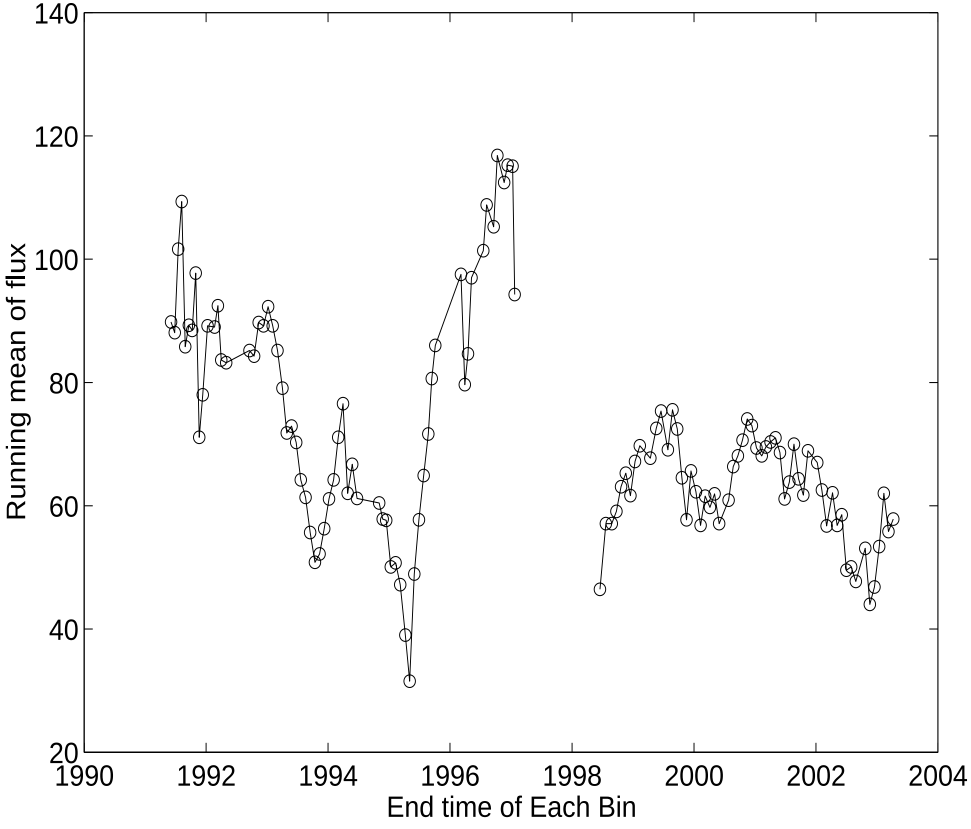

5-point running means of the experimental flux estimates for Gallex and GNO

GALLEX AND GNO DATA ANALYSIS

Likelihood functions for the flux for (a) Gallex and (b) GNO

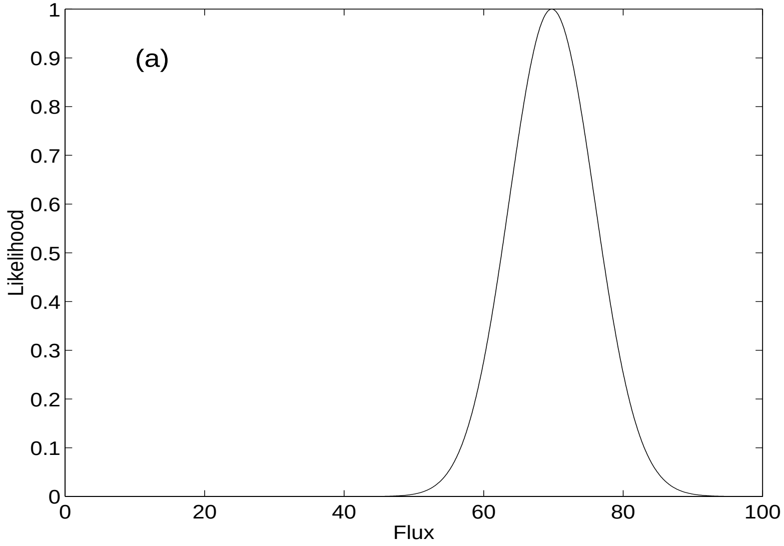

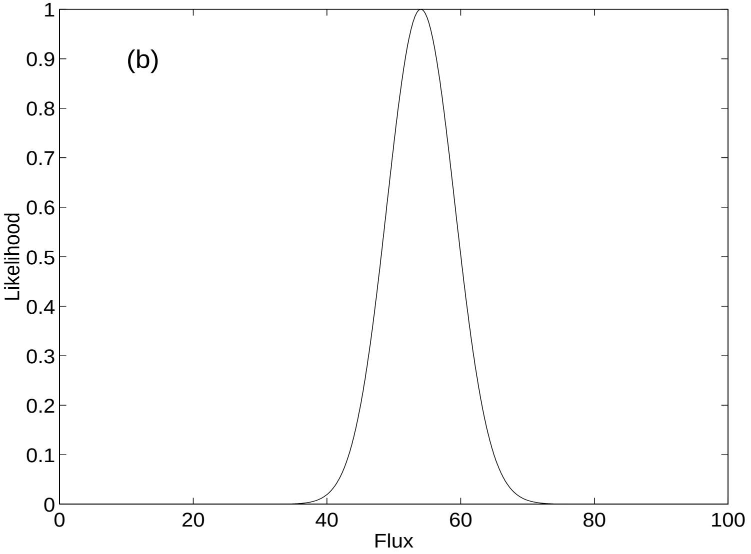

GALLEX $69.9 \pm 6.1\, SNU$ GNO $62.9 \pm 5.4\, SNU$

Flux estimates differ by 2 sigma
P = 0.02

•S0505B04

GALLEX AND GNO DATA ANALYSIS

TABLE 1
GALLEX DATA

Runs	Flux	Upper Error	Lower Error
1 - 13	78.6	18.3	18.1
14 – 26	79.2	14.0	13.9
27 – 39	63.5	12.3	11.9
40 – 52	44.3	10.6	10.1
53 - 65	108.5	16.4	15.6

Chi-Square = 12.77

P = 0.012

Flux Probably Not Constant

TABLE 2
GNO DATA

Runs	Flux	Upper Error	Lower Error
1 - 12	51.3	12.2	11.9
13 Š 23	58.2	12.5	12.1
24 Š 35	72.3	12.3	11.9
36 Š 46	55.4	11.8	11.7
47 - 58	38.5	9.9	9.8

Chi-Square = 4.90

P = 0.29

Flux Probably Constant

•S0505B08

GALLEX AND GNO DATA ANALYSIS

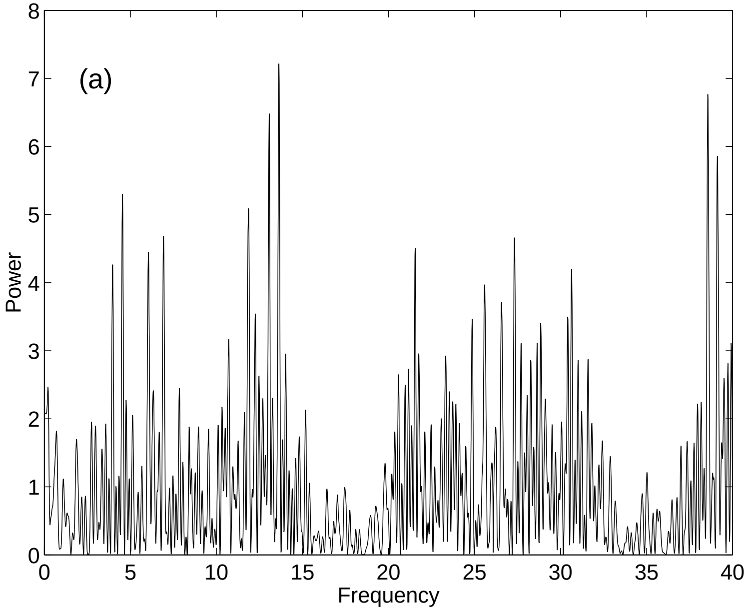

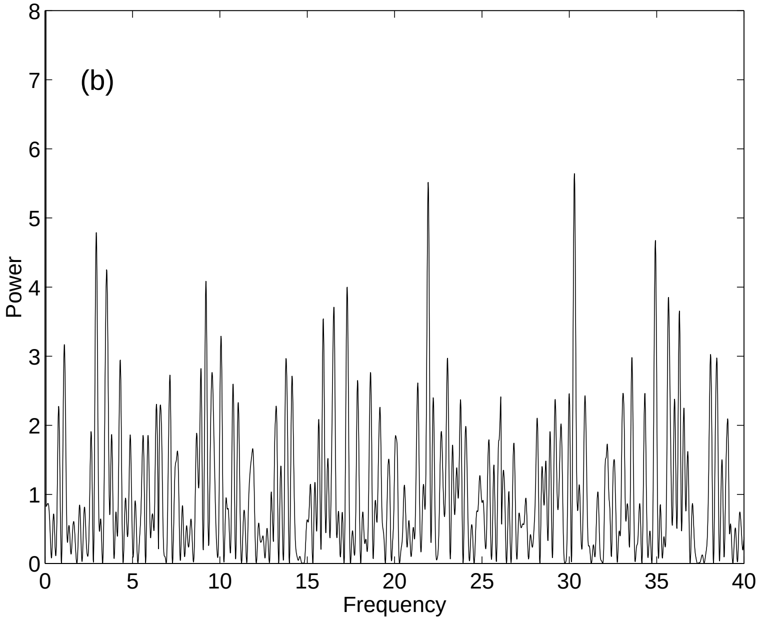

Normalized power spectrum,
calculated using std(g) as the error term, for
(a) Gallex and
(b) GNO.

•S0505B05

JOINT SPECTRUM STATISTIC

From two (or more) power spectra, form a statistic analogous to a correlation statistic, defined so that it is distributed in the same way as a power spectrum.
For gaussian random noise,

$$P(S)dS = e^{-S}dS \quad and \quad P_{>S}(S) = e^{-S}$$

If $Z = S_1 S_2,$ then

$$P(Z)dZ = \int_0^\infty dx \int_0^\infty dy e^{-x-y} \delta(Z - xy) dZ$$

We find that

$$P_{>J}(J) = e^{-J}$$

if

$$J = \ln\left[2Z^{1/2} K_1\left(2Z^{1/2}\right)\right]$$

GALLEX AND GNO DATA ANALYSIS

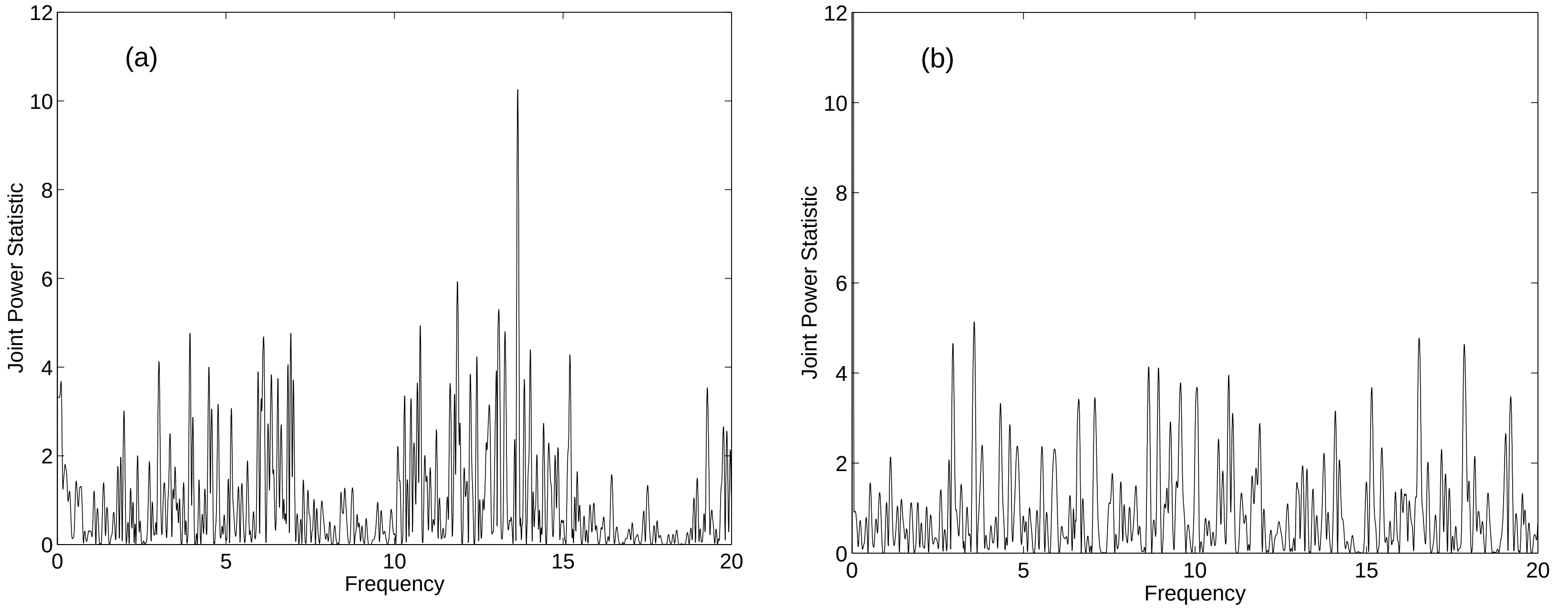

Joint power spectrum formed from power at *nu* and at *2nu* for

(a) Gallex and

(b) GNO.

•S0505B07

R-MODES

In a rotating fluid sphere, r-modes comprise oscillations for which the motion is mainly latitudinal.

In the rotating frame, the oscillation frequencies are given by

$$\nu(l,m) = \frac{2m\nu_R}{l(l+1)}$$

where ν_R is the rotation frequency, $l \geq 2$,
and *l* and *m* are the usual spherical harmonic indices. (The frequencies are independent of the index *n*.)

Consider $\nu_R = 14\,y^{-1} = 444\,nHz$ and $l = 3$. Then

for $m = 1$, $\nu = 2.33\,y^{-1}$ so $P = 157\ days$,

for $m = 2$, $\nu = 4.67\,y^{-1}$ so $P = 78\ days$,

for $m = 3$, $\nu = 7.00\,y^{-1}$ so $P = 52\ days$.

These frequencies are close to the periods of Rieger-type oscillations.

TABLE 3

		Gallex	Gallex	GNO	GNO
		Frequency	Power	Frequency	Power
Rotation, fundamental	12.50 to 13.80	13.07 13.64	6.48 7.22		
Rotation, harmonic	25.00 to 27.60	27.32	4.66		
R-modes, 2-1 and 3-2	4.50 to 4.93	4.54	5.30		
R-mode, 2-2	9.04 to 9.87			9.20	4.25
R-mode, 3-1	2.25 to 2.46				
R-mode, 3-3	6.75 to 7.40	6.93	4.68		

•S0505B09

HOMESTAKE AND GALLEX-GNO

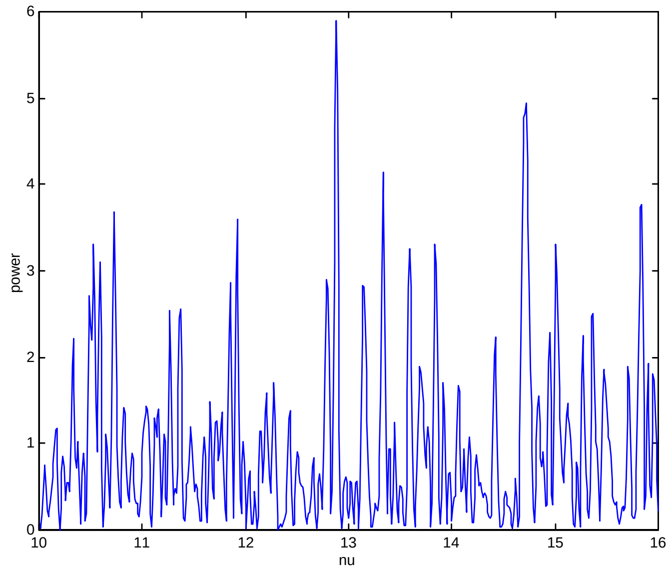

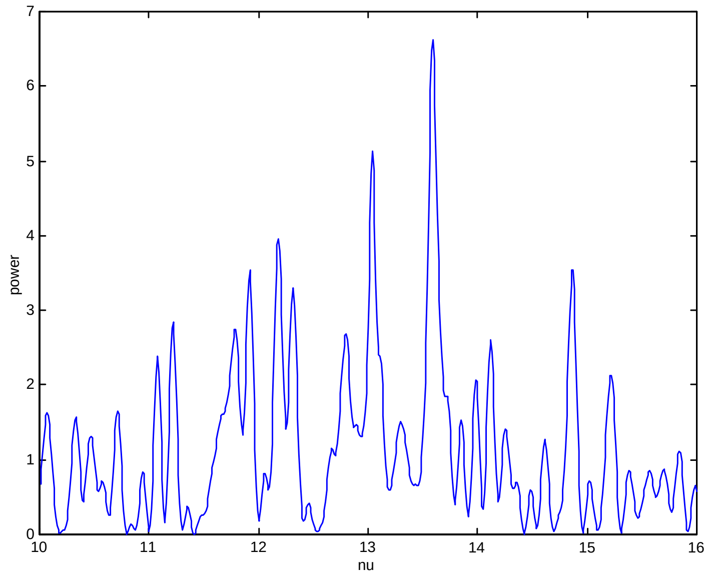

- Lomb-Scargle spectrum of Homestake (left) and GALLEX-GNO (right) data in range 10 – 16 y-1

SXT X-RAY DATA

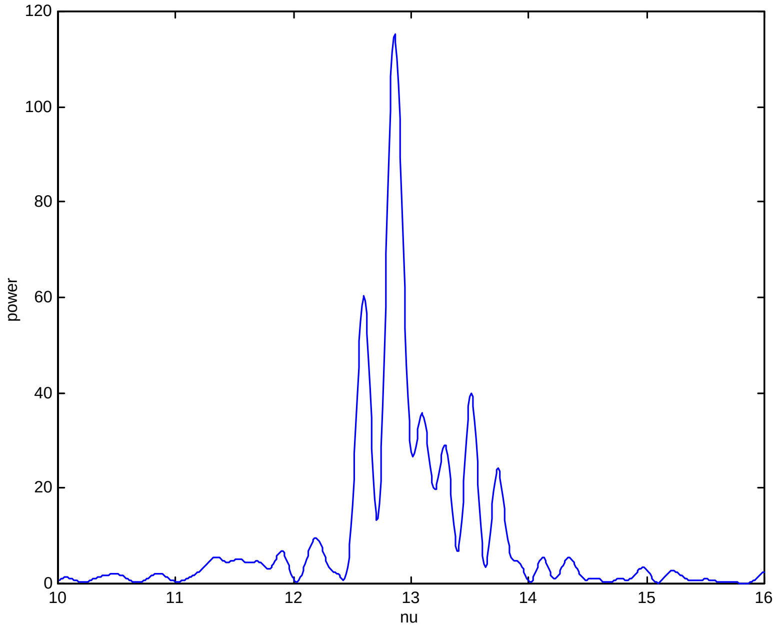

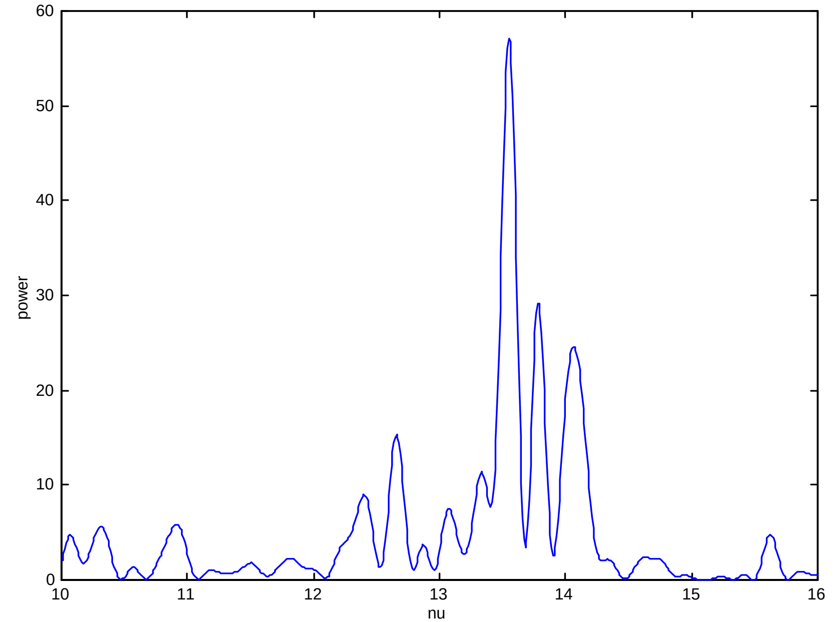

- Power spectra for SXT latitudes N60 and S60 (left) and Equator (right)

NEUTRINO AND X-RAY FLUX SPECTRA COMPARED

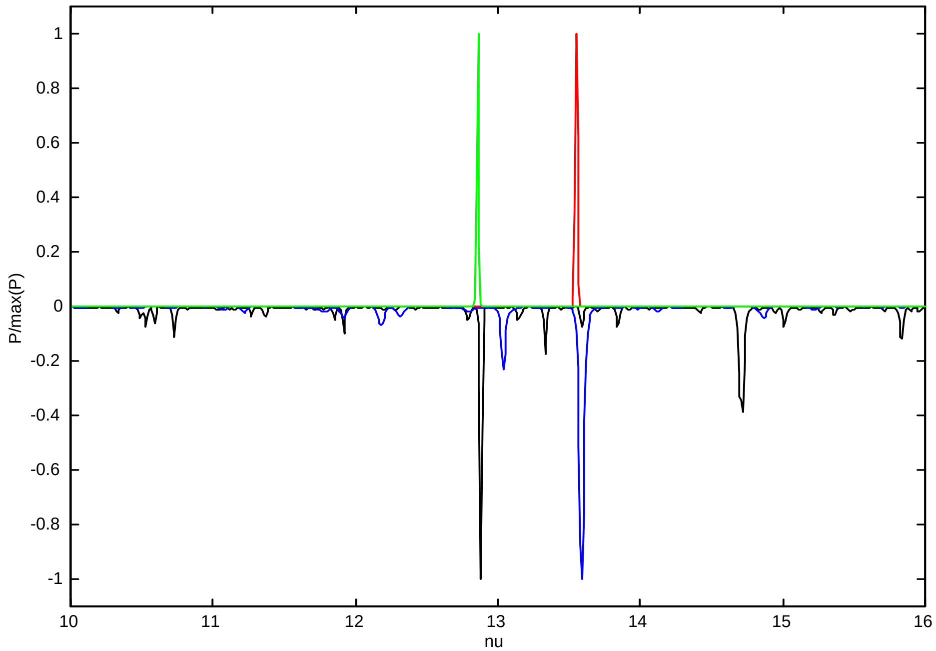

Comparison of normalized probability distribution functions formed from power spectra:

SXT N60&S60 (green), SXT Equator (red),

Homestake (black), and GALLEX-GNO (blue)

SUPER-KAMIOKANDE

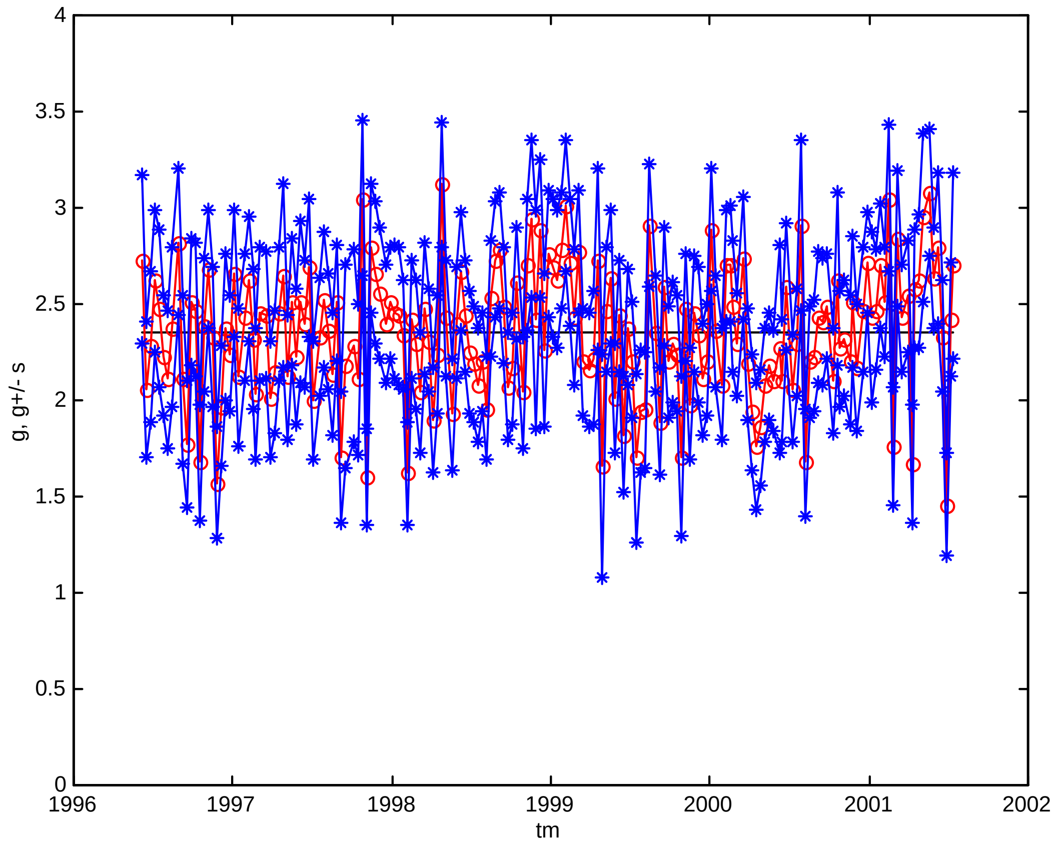

Flux and Error Estimates in 10-day bins

SUPER-KAMIOKANDE, 10-day bins

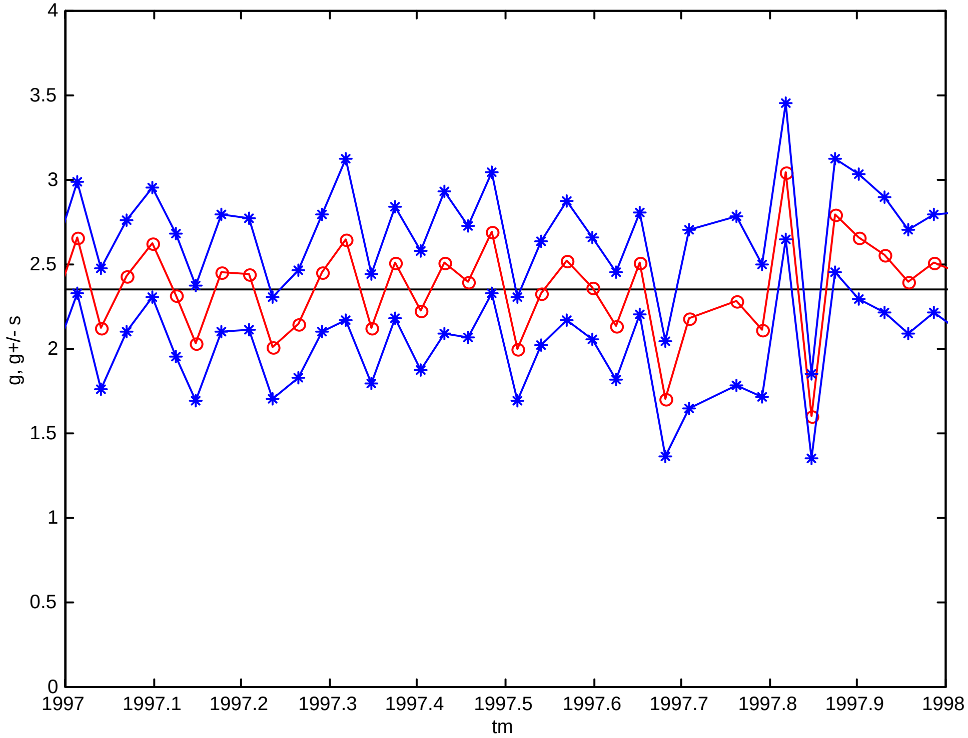

Flux and Error Estimates (One Year Section)

SUPER-KAMIOKANDE, 10-day bins

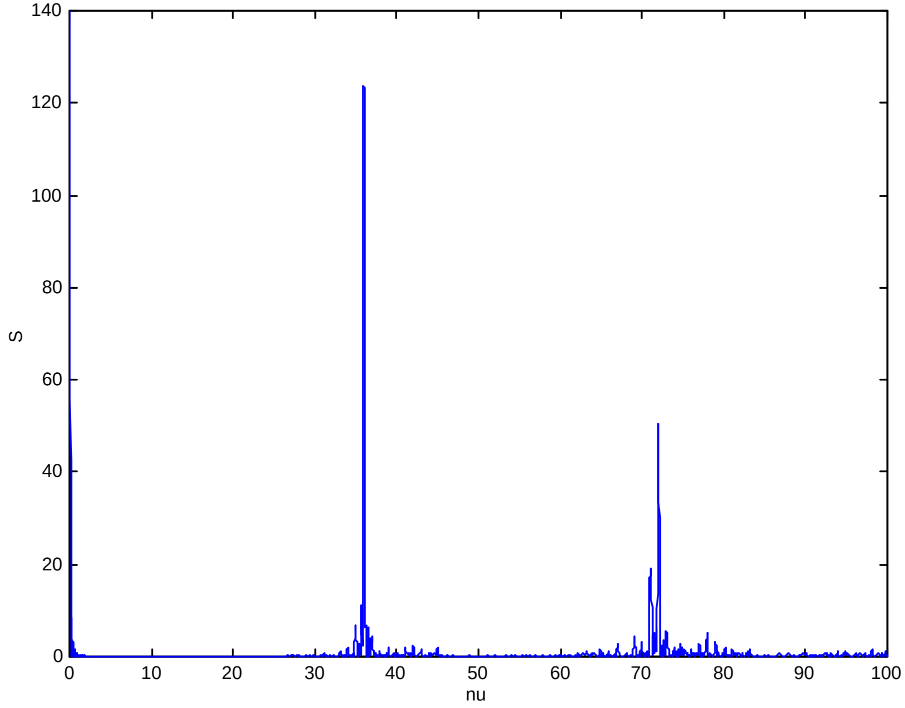

Power Spectrum formed from Timing Schedule
Very Strong Periodicity at 35.98 cpy

SUPER-KAMIOKANDE, 10-day bins

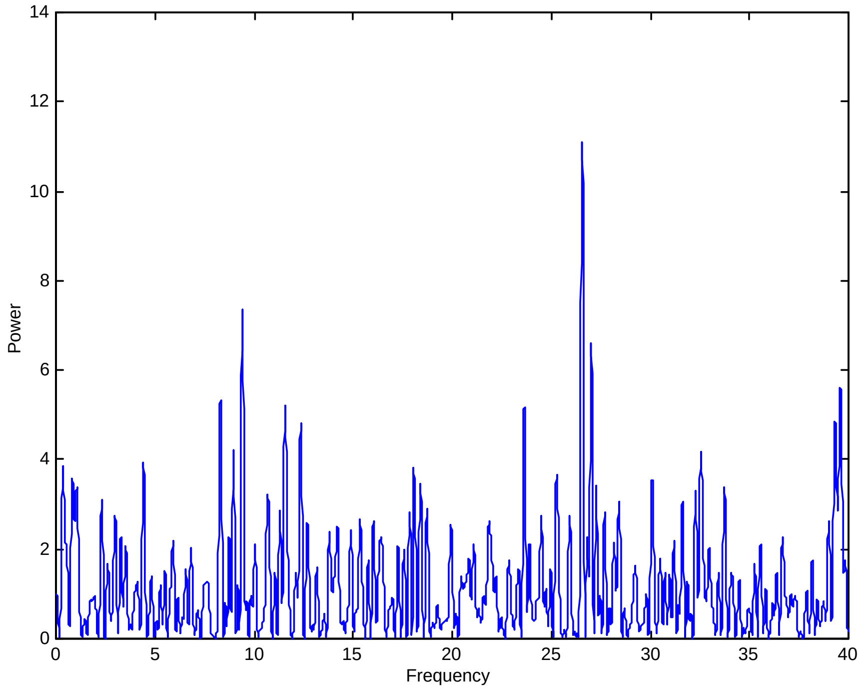

Power spectrum formed by likelihood analysis

The biggest peak is at ν = 26.57 with S = 11.11

The second biggest peak is at ν = 9.41 with S = 7.33

The latter is an alias of the former, due to the peak at 35.98 in the power spectrum of the sampling schedule

SUPER-KAMIOKANDE, 5-day bins

LOMB-SCARGLE ANALYSIS

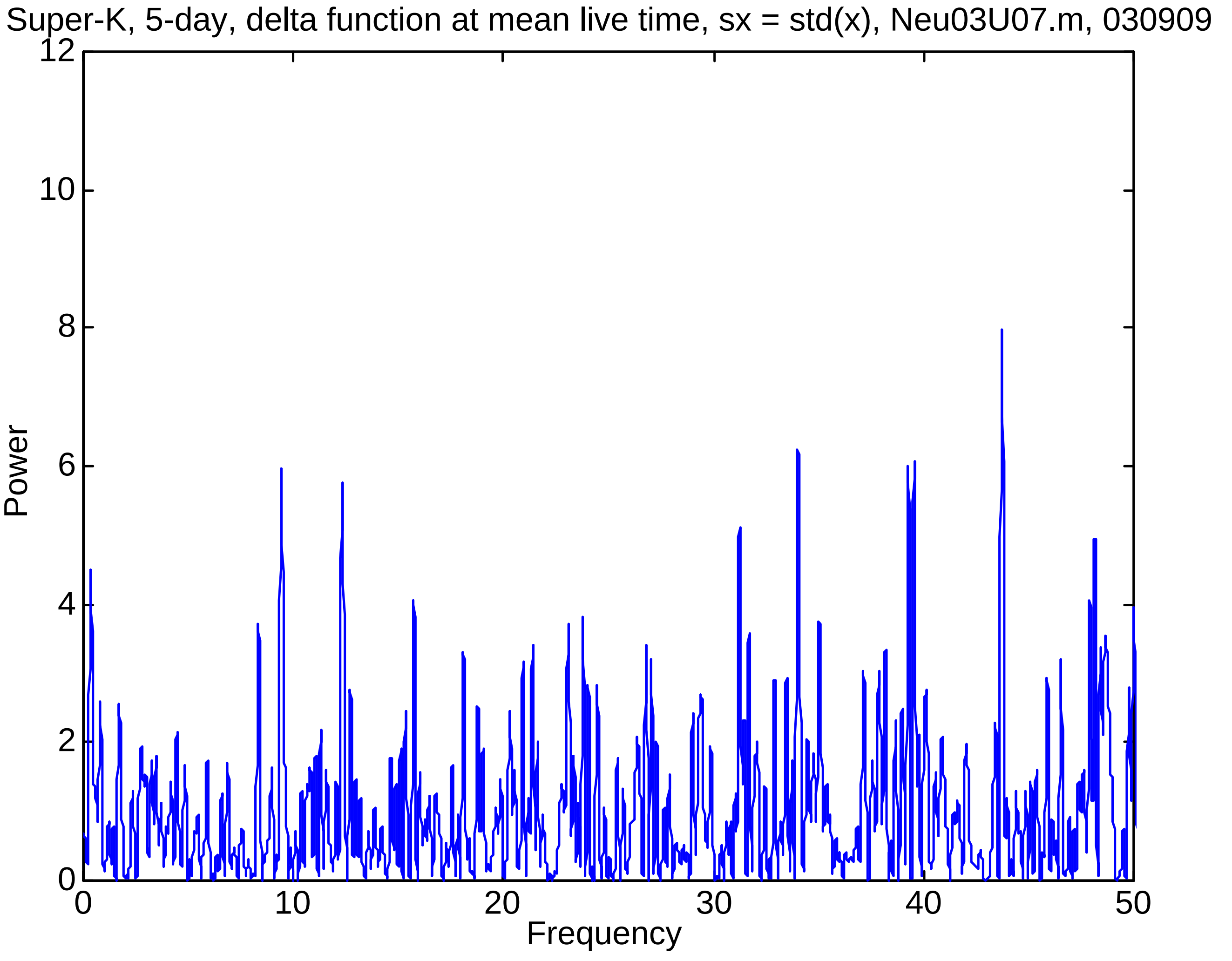

SUPER-KAMIOKANDE, 5-day bins

LIKELIHOOD ANALYSIS

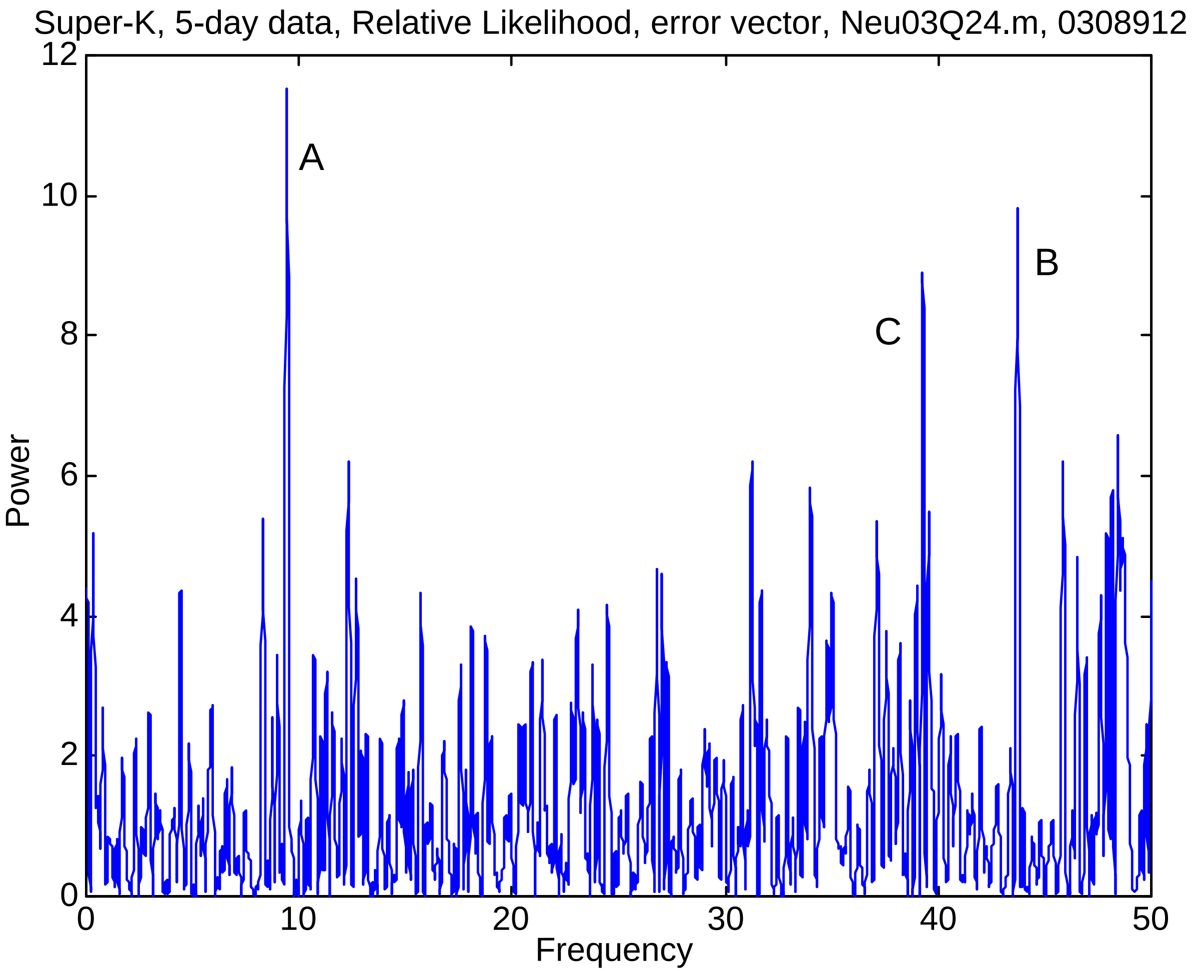

SUPER-KAMIOKANDE POWER SPECTRUM ANALYSIS

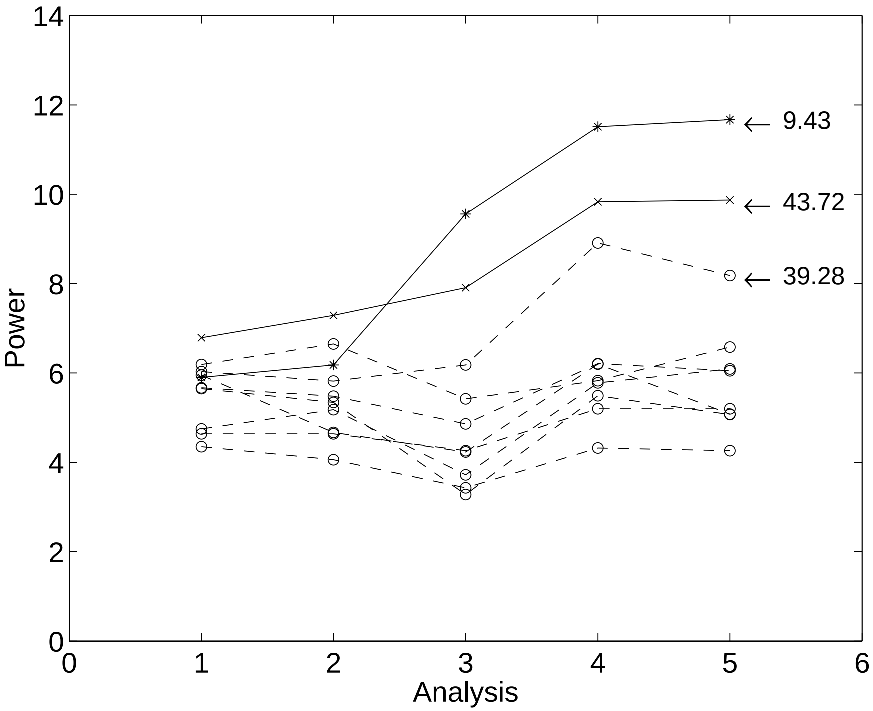

Comparison of powers of top ten peaks for five analysis procedures:
(1) basic Lomb-Scargle analysis, mean times;
(2) basic Lomb-Scargle analysis, mean live times;
(3) modified Lomb-Scargle analysis, mean live times, error data;
(4) SWW likelihood method, start times, end times, and error data;
(5) SWW likelihood method, start times, end times, mean live times, and error data.
Only the peaks at 9.43 yr^{-1} and 43.72 yr^{-1} show a monotonic increase in power.

SUPER-KAMIOKANDE, 5-day bins

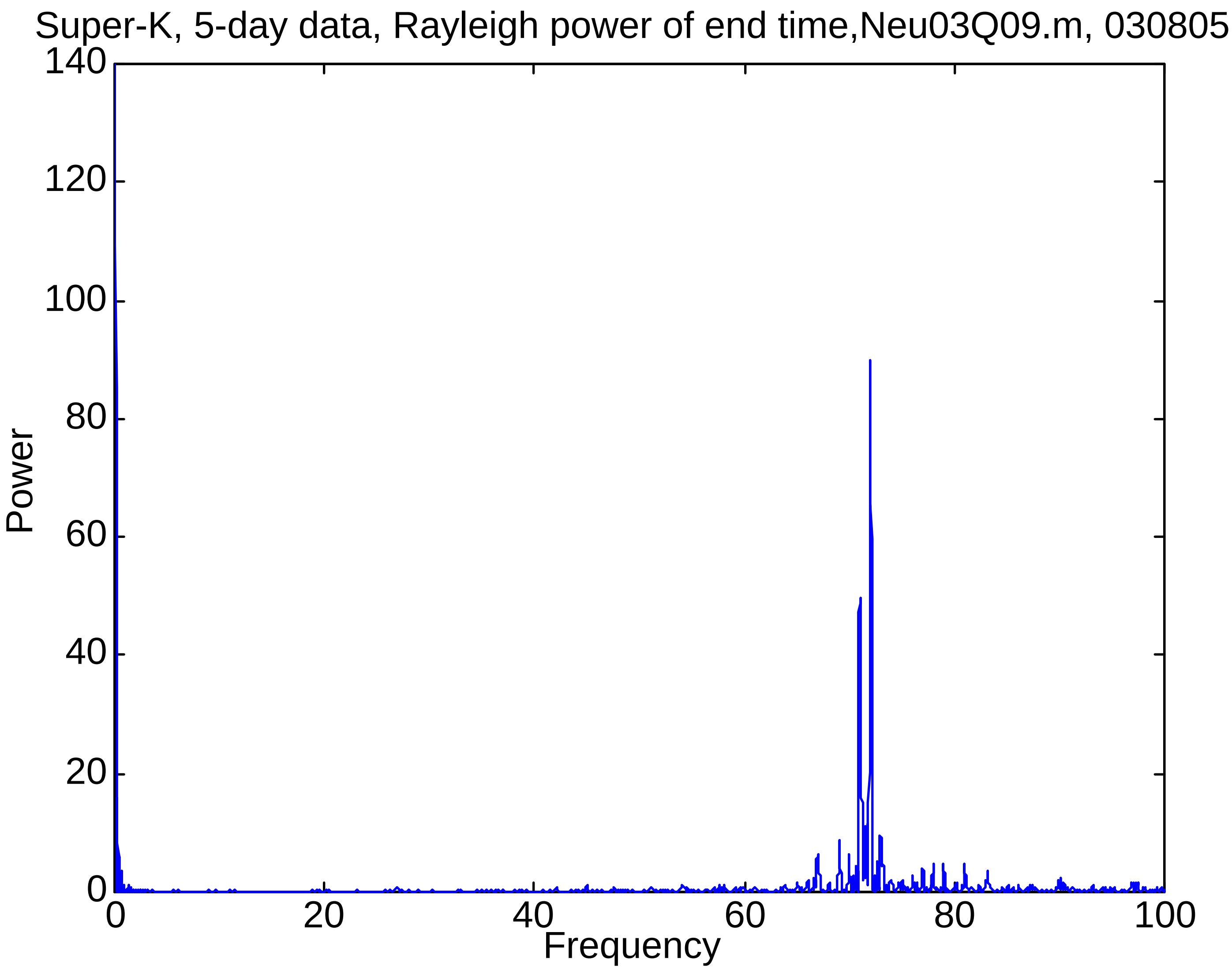

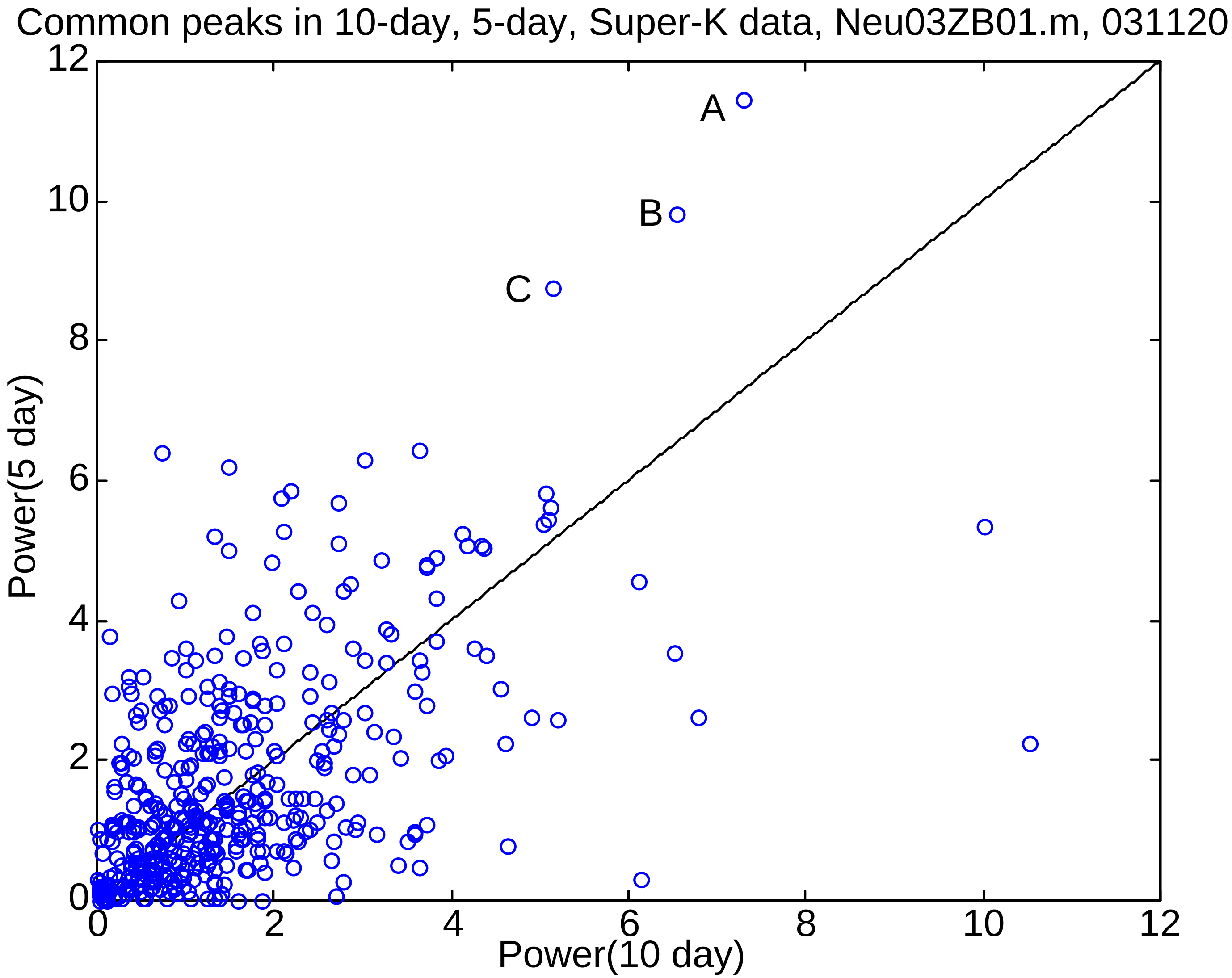
Common peaks in 10-day, 5-day, Super-K data, Neu03ZB01.m, 031120
Power(5 day)
Power(10 day)
A
B
C
0
2
4
6
8
10
12

SUPER-KAMIOKANDE, 5-day bins

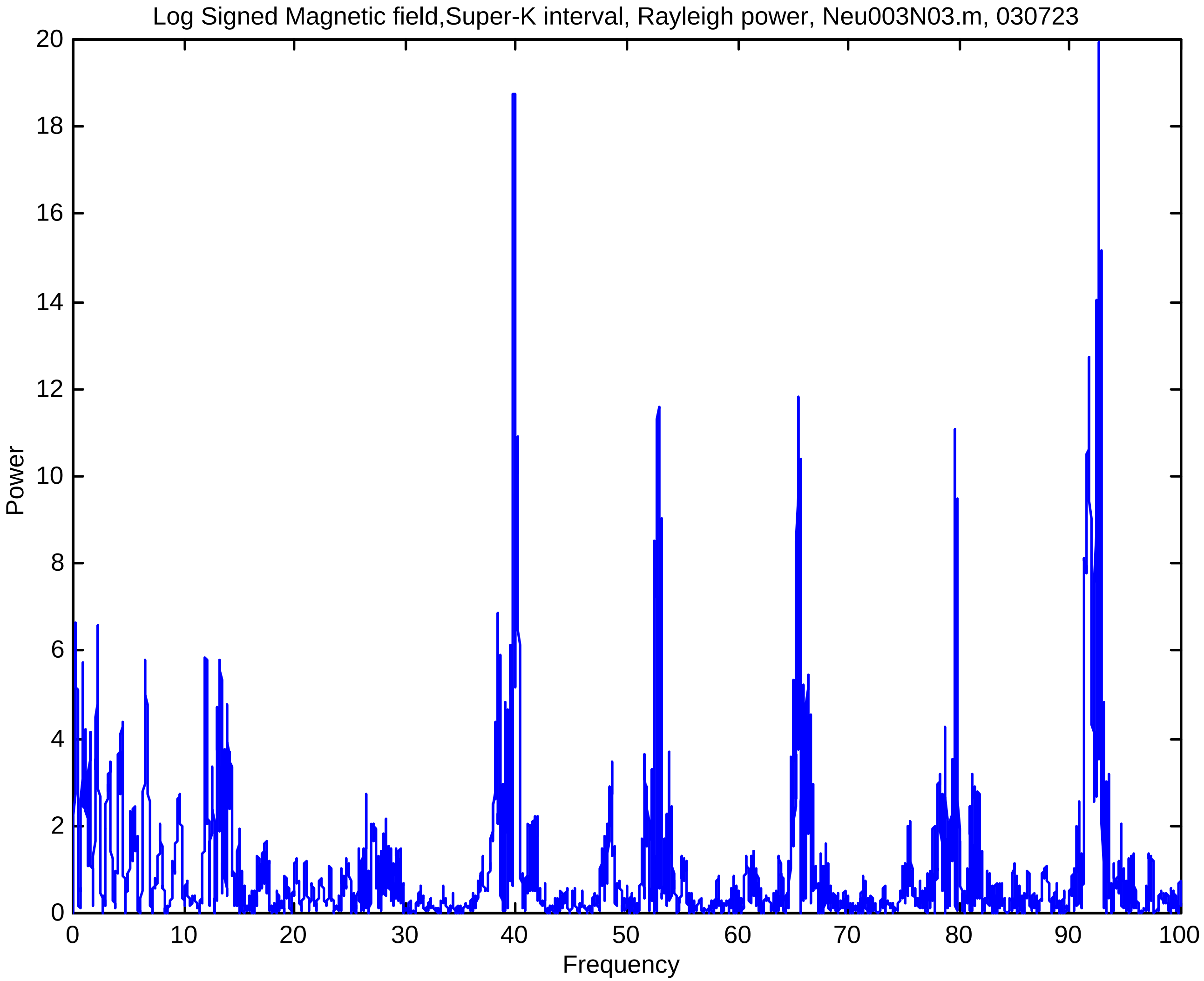

It is therefore interesting to compare the power spectrum of the neutrino measurements with the power spectrum of the magnetic field at Sun center for the period of operation of Super-Kamiokande. We obtain the estimate 13.20 +/- 0.14 for the synodic rotation frequency (or 14.20 +/- 0.14 for the sidereal rotation frequency) of the magnetic field. This leads to the band 39.60 +/- 0.42 for the third harmonic of the synodic rotation frequency of the magnetic field. We see that peak C falls within this band. When we apply the shuffle test (Bahcall & Press 1991; Sturrock,Walther, &Wheatland 1997), randomly re-assigning flux and error measurements (kept together) to time bins, we find that only 5 cases out of 1,000 yield a power 8.91 or larger in the search band .

SUPER-KAMIOKANDE, 5-day bins

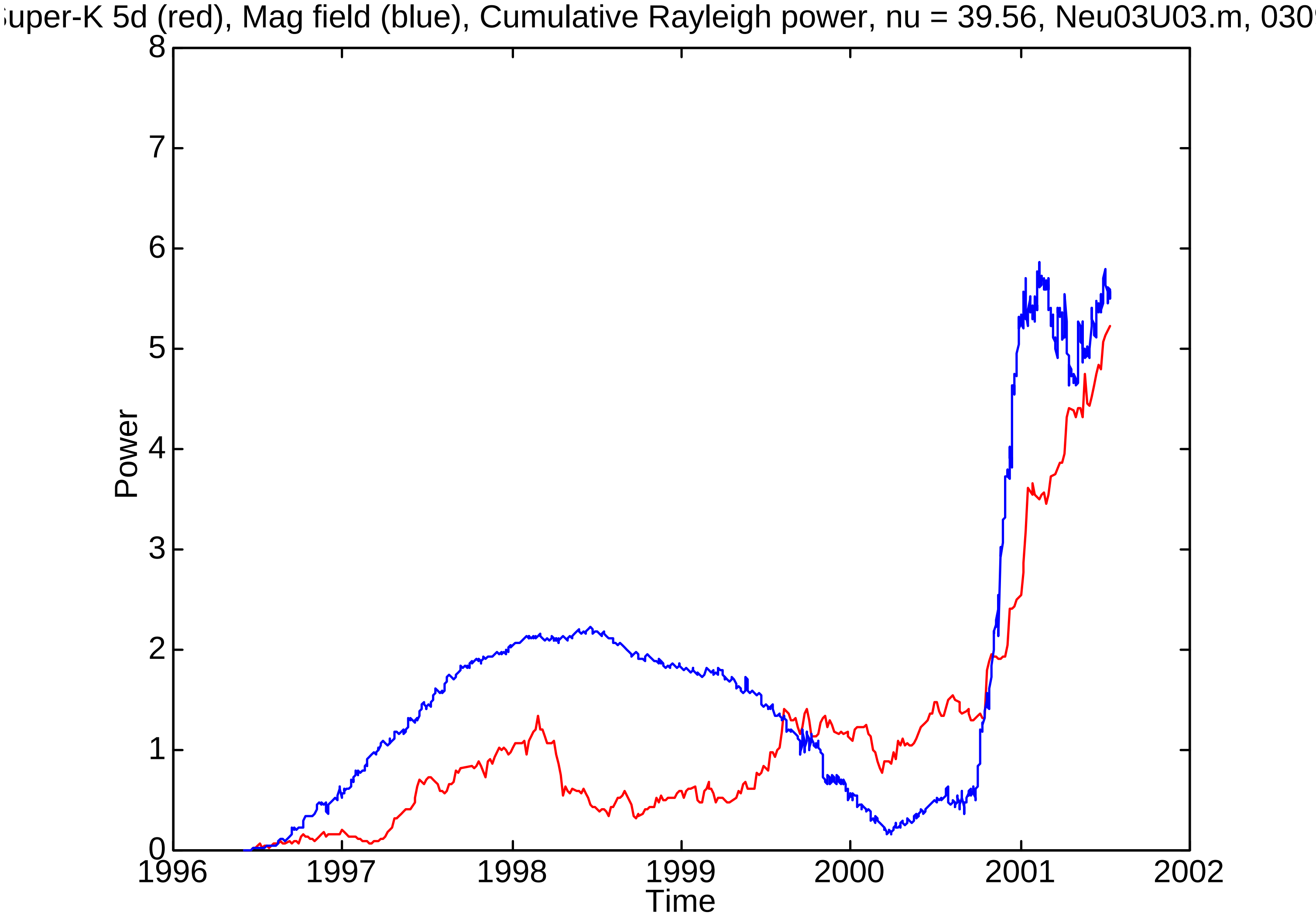

R-modes are retrograde waves that, in a uniform and rigidly rotating sphere, have frequencies

$$\nu(l,m,syn) = m(\nu_R - 1) - \frac{2m\nu_R}{l(l+1)}$$

as seen from Earth, where *l* and *m* are two of the usual spherical-harmonic indices, and *nu* is the sidereal rotation frequency.

An observer co-rotating with the sphere would detect oscillations at the frequency

$$\nu(l,m,rot) = \frac{2m\,\nu_R}{l(l+1)} \qquad (1)$$

Since the mode frequency does not depend upon the radial index *n*, it seems likely that similar oscillations, with similar frequencies, could occur in thin spherical shells inside a radially stratified sphere.

R-mode oscillations may modulate the solar neutrino flux by moving magnetic regions in and out of the path of neutrinos propagating from the core to the Earth. The resulting oscillations in the neutrino flux would be formed from combinations of the frequency with which an r-mode oscillation intercepts the core-Earth line and the frequency with which a magnetic structure intercepts the core-Earth line. These combinations will have the form

$$\nu = \left| m(\nu_R - 1) - \frac{2m\nu_R}{l(l+1)} \pm m'(\nu_R - 1) \right| \qquad (2)$$

Where m' , the azimuthal index for the magnetic structure, may be different from that of the r-mode.

For *m'* = *m* and for the minus sign, this yields the frequency of equation (1), and for the plus sign it yields

$$\nu(l,m,alias) = 2m(\nu_R - 1) - \frac{2m\nu_R}{l(l+1)} \qquad (3)$$

We may refer to this frequency for convenience as an "alias" of the frequency given by equation (1).

VARIABILITY OF THE SOLAR NEUTRINO FLUX

For $l = 2$ and $m = 2$, and for the range of values of inferred from the magnetic-field data, we find that equation (1) leads us to expect an oscillation in the band 9.47 +/- 0.09, and equation (3) leads us to expect an oscillation in the band 43.33 +/- 0.47.

We see that the peaks A and B fall within these two bands.

On applying the shuffle test, we find only 6 cases out of 10,000 in which a peak with power 11.51 or larger occurs in the band 9.47 +/- 0.09, and only 5 cases out of 1,000 that yield a power 9.83 or larger in the band 43.33 +/- 0.47 .

SUPER-KAMIOKANDE, 5-day bins

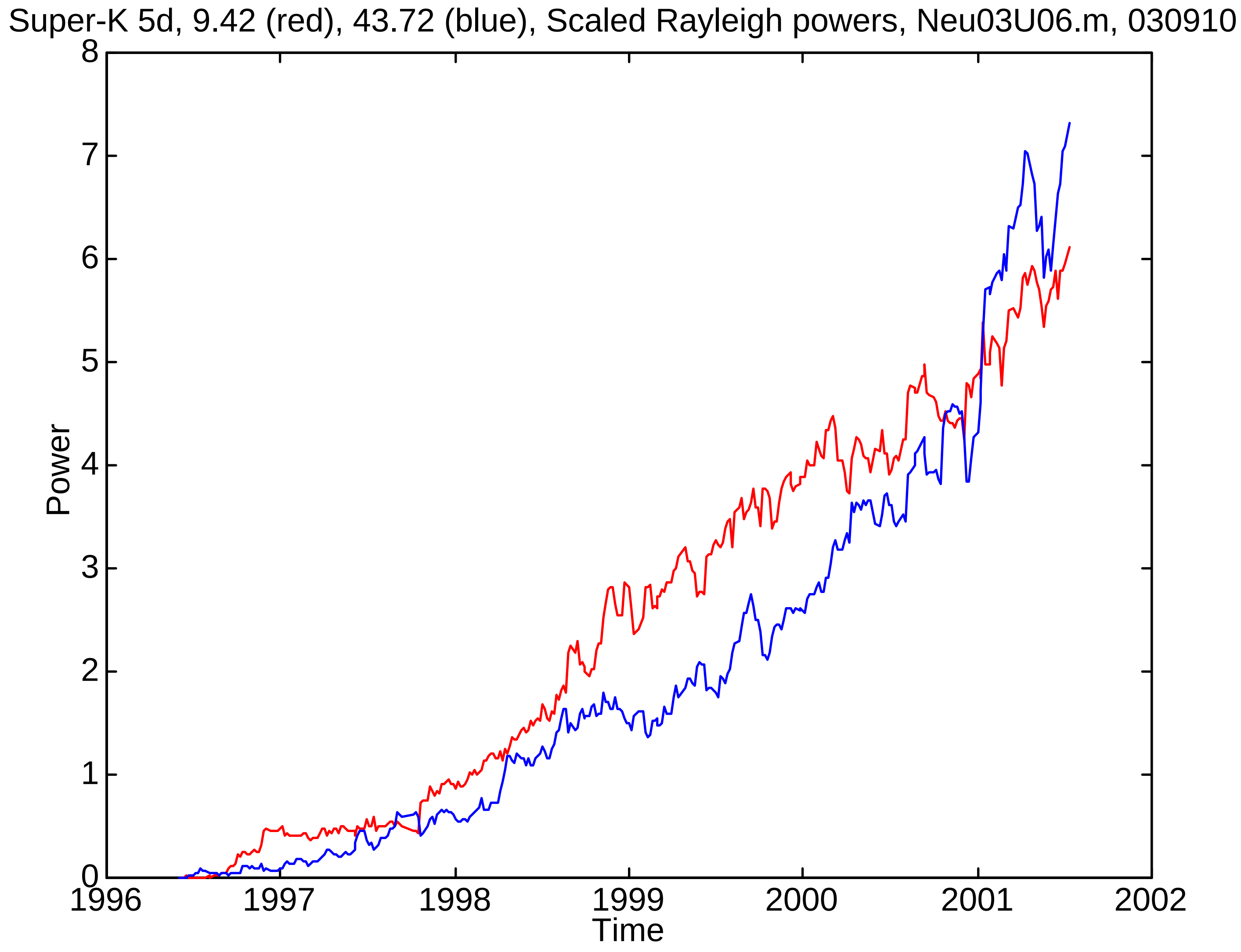

INTERPRETATION OF SOLAR FLUX MODULATION

Super-Kamiokande and SNO data show that Matter-Enhanced Neutrino Oscillations occur

$$\nu_e \rightarrow \nu_{mu} \text{ or } \nu_{tau}$$

This must be the dominant process

KamLAND data imply that similar oscillations occur involving $\overline{\nu}_e$ rather than ν_e

Solar and reactor data can be matched with

$$\Delta m^2 \sim 10^{-4}\, eV^2$$

Time-variation of the solar flux must therefore be a sub-dominant process.

INTERPRETATION OF SOLAR FLUX MODULATION

Time-variation points to the involvement of magnetic field.

This indicates that modulation must be due to

Resonant Spin Flavor Precession (RSFP)

One possibility (Balantekin, Volpe) is

$$\nu_e \rightarrow \bar{\nu}_{mu} \text{ or } \bar{\nu}_{tau}$$

but this effect is weak and occurs in the radiative zone.

To get the correct shape of the time-averaged neutrino energy spectrum, we need

$$\Delta m^2 \sim 10^{-8}\, eV^2$$

The process cannot involve the three active neutrinos, since the width of the Z^0 resonance limits the number of light, active neutrinos to three.

Solar and reactor data require

$$\Delta m^2 \sim 10^{-4}\ eV^2$$

Atmospheric $\nu_{mu} \to \nu_{tau}$ data require $\Delta m^2 \sim 10^{-3}\ eV^2$

Hence a fourth neutrino is required.

This must be sterile, to be consistent with Z^0 data.

Caldwell has proposed that solar-neutrino-flux time variation may be attributed to an RSFP process by which electron neutrinos are converted to sterile anti-neutrinos:

$$\nu_e \rightarrow \bar{\nu}_s$$

via a transition magnetic moment.
The sterile neutrino does not mix with other neutrinos, so this proposal is compatible with all limitations on sterile neutrinos.

This model has been analyzed by Chauhan and Pulido.
They find that
• It gives an improved fit to time-averaged flux measurements
• It eliminates an upturn that is expected, but not found, at lower energies in Super-Kamiokande and SNO data
• It yields the correct magnitude of the modulation over the whole energy range
• It yields the correct location of the effect (in the convection zone)

SIGNIFICANCE FOR SOLAR PHYSICS OF THE VARIABILITY OF THE SOLAR NEUTRINO FLUX

•Neutrinos may be used to probe the Sun’s internal magnetic field and internal dynamics

• Variations are probably due to inhomogeneous magnetic structures with field strengths of order 10^5 Gauss in the outer radiative zone, the tachocline, or deep convection zone

• The Rieger and related periodicities are due to internal r-mode oscillations, probably in or near the tachocline

•Neutrino observations may give advance information of the development of the solar cycle